Energy 101 (2016) 202–210

Contents lists available at ScienceDirect

Energy

journal homepage: www.elsevier.com/locate/energy

Flexible pyroelectric generators for scavenging ambient thermal energy and as self-powered thermosensors

Hulin Zhang [a, *], Yuhang Xie [a], Xiaomei Li [a], Zhenlong Huang [a], Shangjie Zhang [a], Yuanjie Su [a], Bo Wu [a], Long He [a], Weiqing Yang [b], Yuan Lin [a, **]

[a] State Key Laboratory of Electronic Thin Film and Integrated Devices, University of Electronic Science and Technology of China, Chengdu, 610054, China
[b] Key Laboratory of Advanced Technologies of Materials (Ministry of Education), School of Materials Science and Engineering, Southwest Jiaotong University, Chengdu, 610031, China

ARTICLE INFO

Article history:
Received 3 August 2015
Received in revised form
28 January 2016
Accepted 1 February 2016
Available online 24 March 2016

Keywords:
Pyroelectric generator
Thermal energy
Self-powered
Thermosensor

ABSTRACT

Wasted heat is one of the most abundant and widely available energy sources in our living environment and industrial activities. A lot of attentions have been paid on harvesting ambient wasted thermal energy. In this work, a flexible PG (pyroelectric generator) based upon a thin PVDF (polyvinylidene fluoride) film has been fabricated. Based on the pyroelectric effect, the PG can harvest thermal energy arising from the time-dependent fluctuating temperature with spatial uniformity. At the temperature change of 50 K, the PG can deliver an open-circuit voltage of 8.2 V and a short-circuit current of 0.8 μA, respectively, with the maximal output power of 2.2 μW on a load of 0.1 MΩ, which can be utilized to directly drive a LCD (liquid crystal display) or LEDs (light emitting diodes), or to charge a commercial capacitor for subsequent usages. Moreover, the PG can be used to construct a self-powered thermosensor as a result of the linear relationship between the output voltage and the temperature change. Our study promotes the development of the PG for scavenging wasted thermal energy and opens up plenty of potential self-powered applications.

1. Introduction

With the rapid development of the human society, energy shortage is becoming more and more serious than ever before. In order to solve the energy crisis, the exploitation of harvesting the ambient energy has attracted the widespread attention. Wasted heat is a very rich energy source, which widely exists in our daily life, including automotive internal combustion engines, industrial wasted water, household water and so on. It would be a green and renewable energy source if wasted heat could be harvested and reused.

Generally, harvesting thermal energy mainly relies on the Seebeck effect that uses electrons or holes as the working carriers for heat pumping and electricity generation [1,2]. It is known to all that the existence of a temperature difference between the two ends of the conventional thermoelectric cell is necessary for power generation based on Seebeck effect [3]. However, in the actual environment according to the entropy increase principle, the temperature tends to be spatially uniform without a gradient. It is difficult to achieve a steady and huge temperature difference. As a result, the Seebeck effect is hardly to be efficiently used to convert thermal energy arising from a time-dependent temperature variation with spatial uniformity to electric energy. Furthermore, the energy conversion efficiency of the current thermoelectric devices based upon Seebeck effect is still very low [4]. Therefore, it is necessary to put forward an alternative approach to grab thermal energy from the ambient environment.

Pyroelectric effect is a seldom noticed property in some solid or condensed materials, which is about the temperature-dependent spontaneous polarization in certain anisotropic solids [5,6]. Usually, the bound surface charges induced by the spontaneous polarization are balanced by the free charges adsorbed in the crystal surface. The net bound charges will be obtained once there is a temperature fluctuation due to the change of the polarization

* Corresponding author.
** Corresponding author.
E-mail addresses: zhangd198710@gmail.com (H. Zhang), linyuan@uestc.edu.cn (Y. Lin).

http://dx.doi.org/10.1016/j.energy.2016.02.002
0360-5442/

dipole moment [7]. Nevertheless, there are only a few studies about harvesting thermal energy using pyroelectric effect [8–12]. In these articles, the authors mainly focused on the demonstration of the electricity generation based on the different pyroelectric materials. The output power is the sole concern. However, the related applications based on the pyroelectric generators are hardly involved in these papers. Therefore, it is necessary to develop energetically the related applications based on the generators. We should not only focus on the electricity generation, but also develop an active self-powered sensor by using generators.

Small-scaled electronics or sensors have attracted intensive interest because of their extensive applications in the modern society [13–16]. An electronic thermometer, as one of the most common typical small electronics, is a device that measures a temperature or temperature gradient, mainly based on the thermoelectricity or the infrared radiation [17,18]. Usually, an external power is indispensable to drive these small-scaled sensors. The self-powered technology, proposed by Dr. Zhong Lin Wang at Georgia Tech in 2010, is based on driving sensors by grabbing energy from the ambient environment instead of conventional batteries or other external power sources [19,20]. This implies that it may be feasible by using the PG (pyroelectric generator) as a self-powered thermosensor that proactively detects ambient temperature without using any external power sources, which can radically improve the adaptability and mobility of such sensors. Even so, there are few reports about using a PG based on the PVDF (polyvinylidene fluoride) as a self-powered thermometer.

In this paper, a flexible PG was fabricated by using a PVDF film for harvesting thermal energy resulting from the time-dependent temperature fluctuation based on the pyroelectric effect. The designed PG can be used as a direct power source for lighting up a LCD (liquid crystal display) or commercial LEDs (light emitting diodes). Furthermore, it is demonstrated that the PG can be employed as an active self-powered thermometer to detect the ambient temperature. This research will push the development and applications of the PG-based small electronics in thermal energy harvesting, self-powered sensing, and others.

2. Experimental details

2.1. Fabrication of a PG device

A PVDF film with the thickness of 120 μm was deposited with a 15 μm thick Al layer on its top and bottom surface. The two Al layers were employed as the electrodes, which connected to the measuring systems or external electrical appliances.

2.2. Electric output measurement

While measuring the electrical output performance, the PG was attached on a heater, where the temperature could be controlled accurately and monitored by using a thermometer. The output signals, including voltage and current, were measured by an Agilent B2901A system.

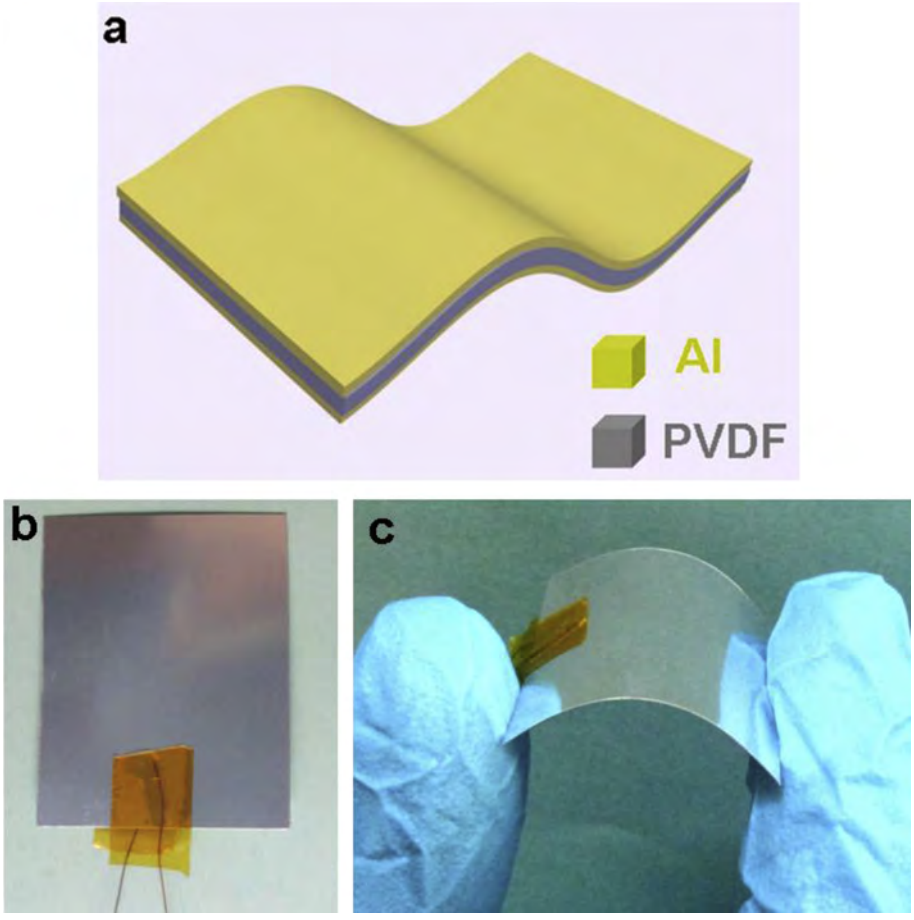

Fig. 1. Device structure of a PG. (a) The schematic diagram. (b) Photograph of the constructed PG. (c) Image of the bent PG.

2.3. Demonstration of the self-powered thermosensor

When demonstrating the potential applications of the PG as an active self-powered thermosensor, the PG was still fixed on the heater, which served as the detected heat source. The room temperature was confirmed to be 293 K through out all the experiments.

3. Results and discussion

As depicted in Fig. 1a, the schematic structure of the constructed PG is composed of three layers. The top and bottom Al were deposited as the electrode layers with the interior PVDF thin film being selected as the pyroelectric material. The PVDF film has the thickness of about 120 μm with the uniformly coated Al layers of 15 μm thick. For the convenience of operation, the PG was fabricated with the approximate size of 25 mm × 20 mm, which is illustrated in Fig. 1b. Fig. 1c displays a photograph of the bent PG, illuminating that the PG is flexible. The appropriate flexibility is of importance for electronic devices in certain practical applications, especially in plying-up energy harvesting and sensing.

To verify the thermal-to-electrical energy conversion of the constructed device, the output performance of the PG was investigated here. The temperature variation curve and the corresponding differential curve are plotted clearly in Fig. 2a. The operation range of the temperature is selected from the room temperature (293 K) to 313 K, with the maximal temperature changing rate more than 3 K/s. When the operated PG was connected forward with the measurement instruments, a sharp negative output voltage pulse was observed as well as the resulting current peak as the temperature increased from 293 to 313 K. The corresponding value of the voltage and current can reach 2.4 V and 0.55 μA, respectively, which is illustrated in Fig. 2b. When the temperature recovered back to 293 K, a positive output voltage/current peak was captured. Similarly, under the reversed connection, the opposite voltage/current signals with the approximate value to the forward counterpart were achieved, as is displayed in Fig. 2c, suggesting the recorded output electric signals were produced by the PG. Fig. 2d shows the output voltage and current rectified by a full-wave bridge circuit, which further demonstrate the electricity was indeed generated by the PG device.

To explore the electricity induced by the generator, the output performance of the PG was measured in detail, as is plotted in Fig. 3. Fig. 3a, d, and g present the output open-circuit voltage and short-circuit current of the PG operated at the temperature difference of 10 K, 30 K and 50 K relative to the room temperature, respectively. It is clear to be seen that both the output voltage and current increase with the increasing temperature difference, implying a higher temperature results in a larger output owning to the enhancing changing rate of spontaneous polarization at a larger

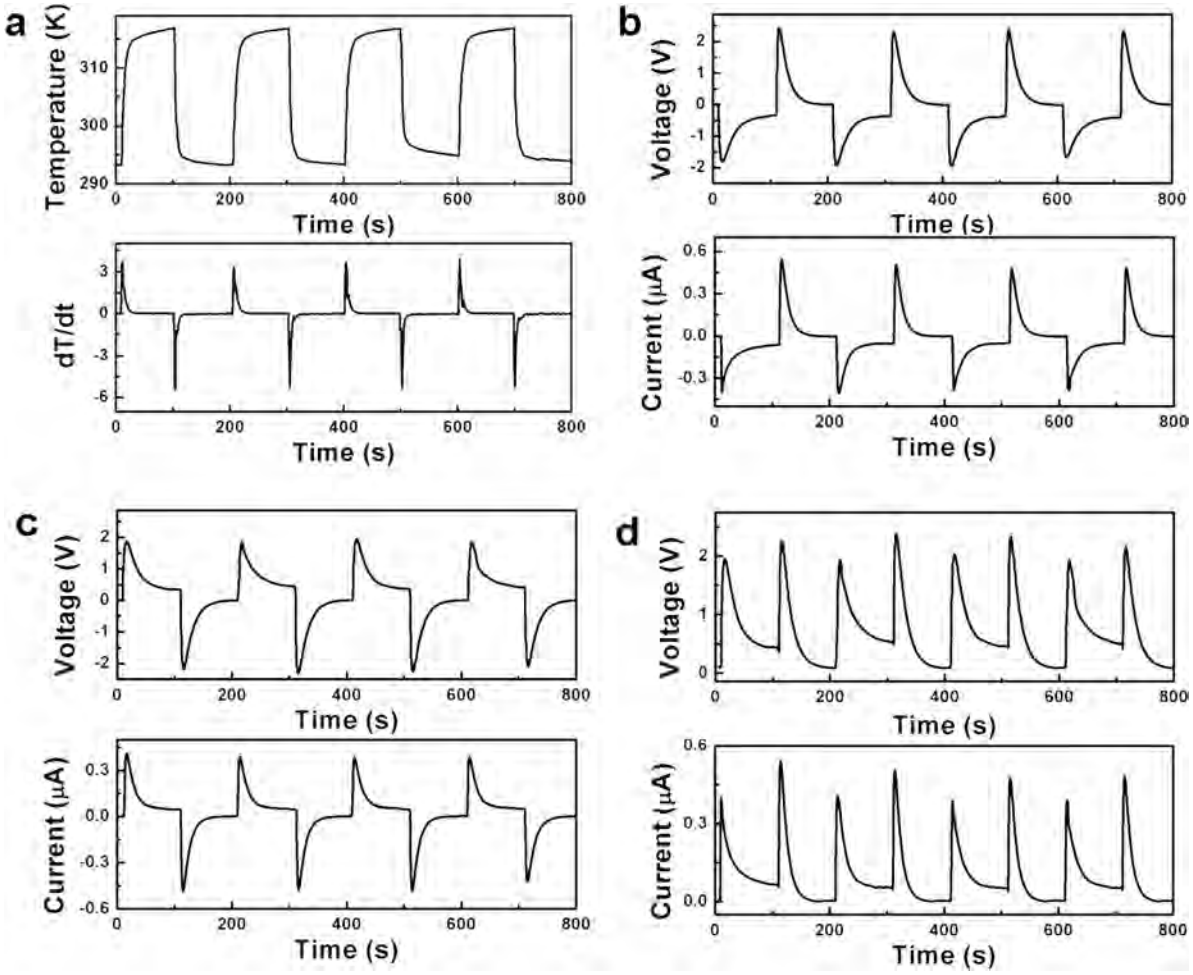

Fig. 2. The output signals of the PG under the cyclic temperature change. (a) The cyclic temperature change of the PG and the corresponding differential curve. (b) The output voltage and current under the forward connection condition. (c) The output voltage and current under the reversed connection condition. (d) The output voltage and current after rectification.

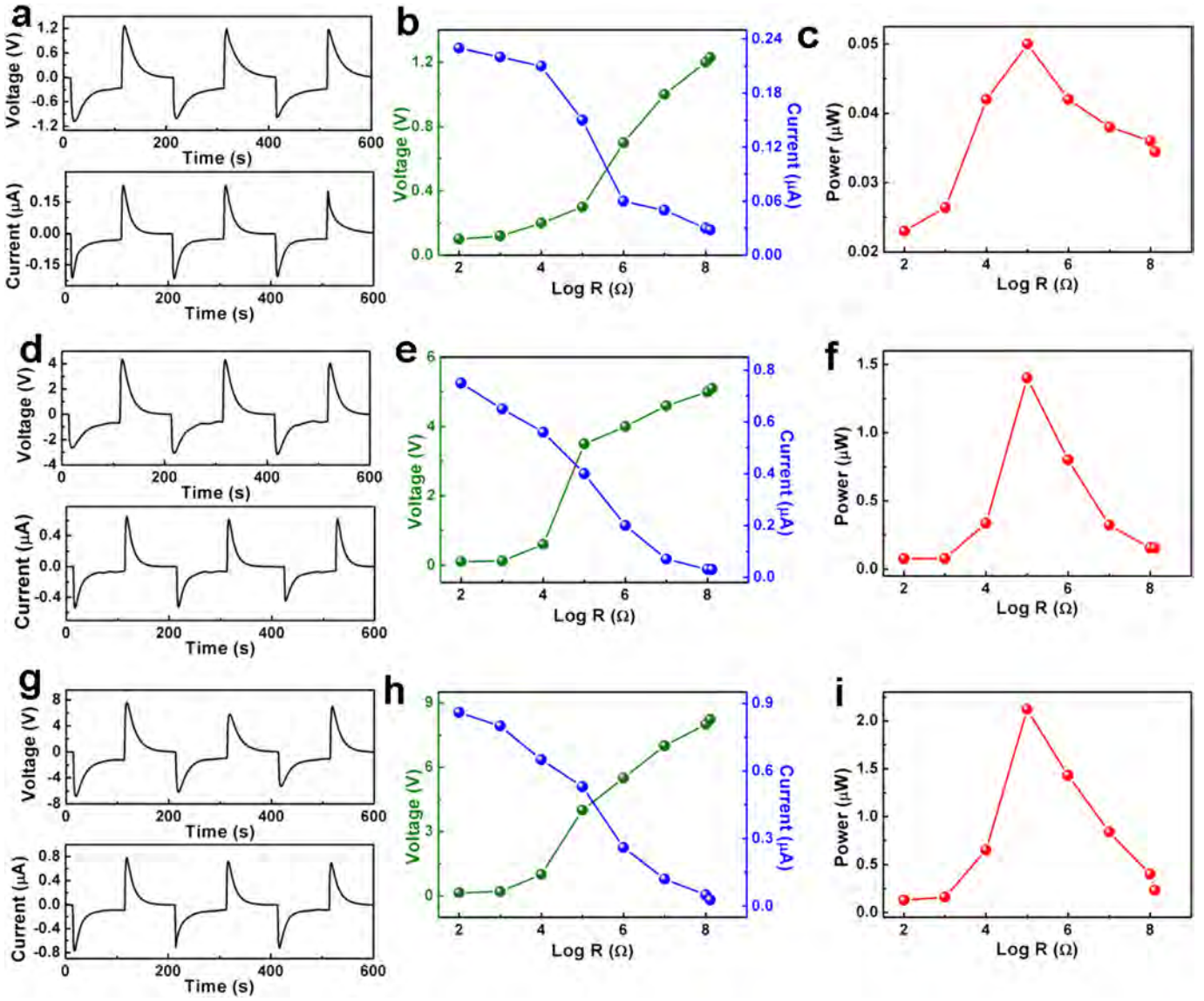

Fig. 3. The output performance of the PG at different temperature differences. (a) The output voltage/current and (b–c) summarized dependence of the voltage, current and power on the load resistance at the temperature difference of 10 K. (d) The output voltage/current and (e–f) summarized relationship between the voltage/current/power, and the load resistance at the temperature difference of 30 K. (g) The output voltage/current and (h–i) summarized dependence of the voltage/current/power on the load resistance at the temperature difference of 50 K.

temperature difference [8,21]. Under the corresponding reversed connection condition, the real-time output voltage and current curves at different temperature differences is opposite, which is depicted in Fig. S1, Supporting information. To further demonstrate the availability of the PG, the output voltage and current at different load resistances were recorded under the various temperature differences. Fig. 3b, d and h exhibit the corresponding output voltage/current as a function of load resistance, indicating the voltage increases while the corresponding current has the reverse trend with the raising load resistance. The dependences of the output power of the PG on the load resistance are shown in Fig. 3c, f and i, respectively. Obviously, the output power ascends at the low external resistance and then descends at a successive higher resistance. At the temperature difference of 50 K, the maximum output power can be achieved of about 2.2 μW at the load resistance of 0.1 MΩ.

To understand the above experimental results, the operation mechanism of the PG is sketched schematically in Fig. 4. The direction of the spontaneous electric dipole in molecules is quite susceptible to the molecular thermal motion which depends on the temperature. According to the principles of thermodynamics, all dipoles would have the same orientation without wobbling at the temperature approaching absolute zero under the ideal condition. The dipoles would wobble random around respective polarization equilibrium axis once the temperature changes. Meanwhile, the larger wobbling angle corresponds to the higher temperature [8,22]. The total average intensity of the spontaneous polarization from the dipoles is constant when temperature is invariable. As a result, there is no output current observed in the external circuit under the condition of $dT/dt = 0$ (Fig. 4b). When a higher temperature is applied on the PG, the dipoles oscillate within a larger angle (θ^+) regarding to the original state (θ) due to the increase of the temperature, leading to the decrease of the total average spontaneous polarization [8]. The electrons can flow from the top electrode to the bottom because of the decreasing induced charges in the electrodes, which is illustrated in Fig. 4a. Conversely, if the PG

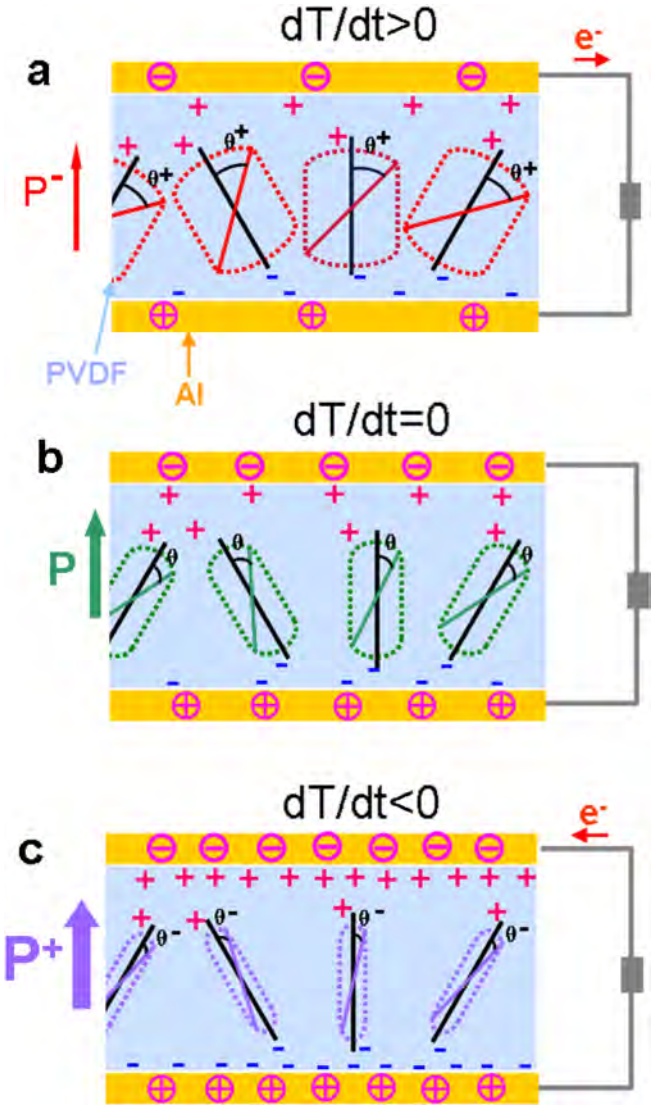

Fig. 4. The proposed typical mechanism of the PG in electricity generation. Sketched diagrams of the PG with negative electric dipoles under (a) the heated, (b) the invariable temperature, and (c) the cooled conditions.

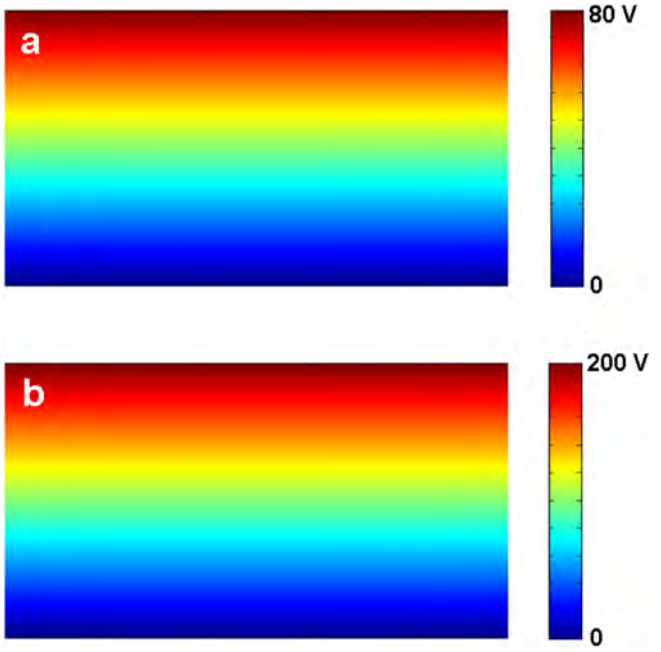

Fig. 5. The simulations of the electrical potential distribution in the PG. (a) The potential distribution of the PG at the temperature difference of 20 K. (b) The potential distribution at the temperature difference of 50 K.

device is cooled instead of being heated, the electric dipoles oscillate within a smaller angle (θ^{-}) on account of the lower thermal motion. Hence, the total polarization is markedly raised and then the increasing induced charges in the electrodes can give rise to a flow of electrons from the bottom electrode to the top, as depicted in Fig. 4c.

The excellent performance of the constructed PG has been achieved due to the change of the total polarization as a result of the temperature fluctuation. In order to give a vivid explanation of the performance, a numerical simulation by the COMSOL software has been established to obtain the electrical potential distribution across the PVDF film subjected with different temperature differences, as illustrated in Fig. 5. The model with the same size as the real deice is employed here and the bottom electrode is connected to ground. Fig. 5a and b shows the pyroelectric potential distribution of the polymer film under the temperature change of 20 K and 50 K, respectively. It is apparent to see that the potential difference between two electrodes can be up to 80 V and 200 V under the respective temperature change, which is obviously much higher than the experimental datum. The disparity between the measurements and simulations implies that the output performance of the PG has a huge margin of improvement.

As is displayed in Fig. 1, the device is consisted of three layers, including two Al electrode layers and a PVDF film. The defects in the PVDF film and Al electrode layer are inevitable, which can visibly damage the electrical property of the materials. The contact between the electrode layers and PVDF film can hardly achieve the perfect contact state. As a result, the amount of the induced charges on the electrodes will not completely equal to that caused by the variation of the total spontaneous polarization. This is the first influence factor of the output performance. In addition, the temperature applied on the PG device is conducted by a heater and the temperature of the PG device is detected by a thermometer. Obviously, the heat applied on the PG device is not homogeneous as well as that the recorded temperature is not precise enough. Meanwhile, the heat transfer on the PG device is not under the ideal condition, where the thickness, structure, interface state and others should be considered. The applied temperature can not be controlled accurately due to the complex interface state, which is another reason. Besides, ambient environment around the PG device can affect the overall electric output performance, which is including thermal, mechanical, chemical, electrical, optical, humid, and other influence factors. In a word, the practical output performance of the PG device is influenced by all the listed and unlisted factors, which is the synthetical result of the multiple actions.

Based on the pyroelectric theory, the pyroelectric current (i_{PG}) can be illustrated as following:

$$i_{PG} = pA\frac{dT}{dt} \tag{1}$$

In this equation, A is the electrode area, which is related to the size of the PG device. p is the pyroelectric coefficient that is a constant for a certain material, as well as with dT/dt indexed to the temperature variation rate. According to the fitting for the recorded

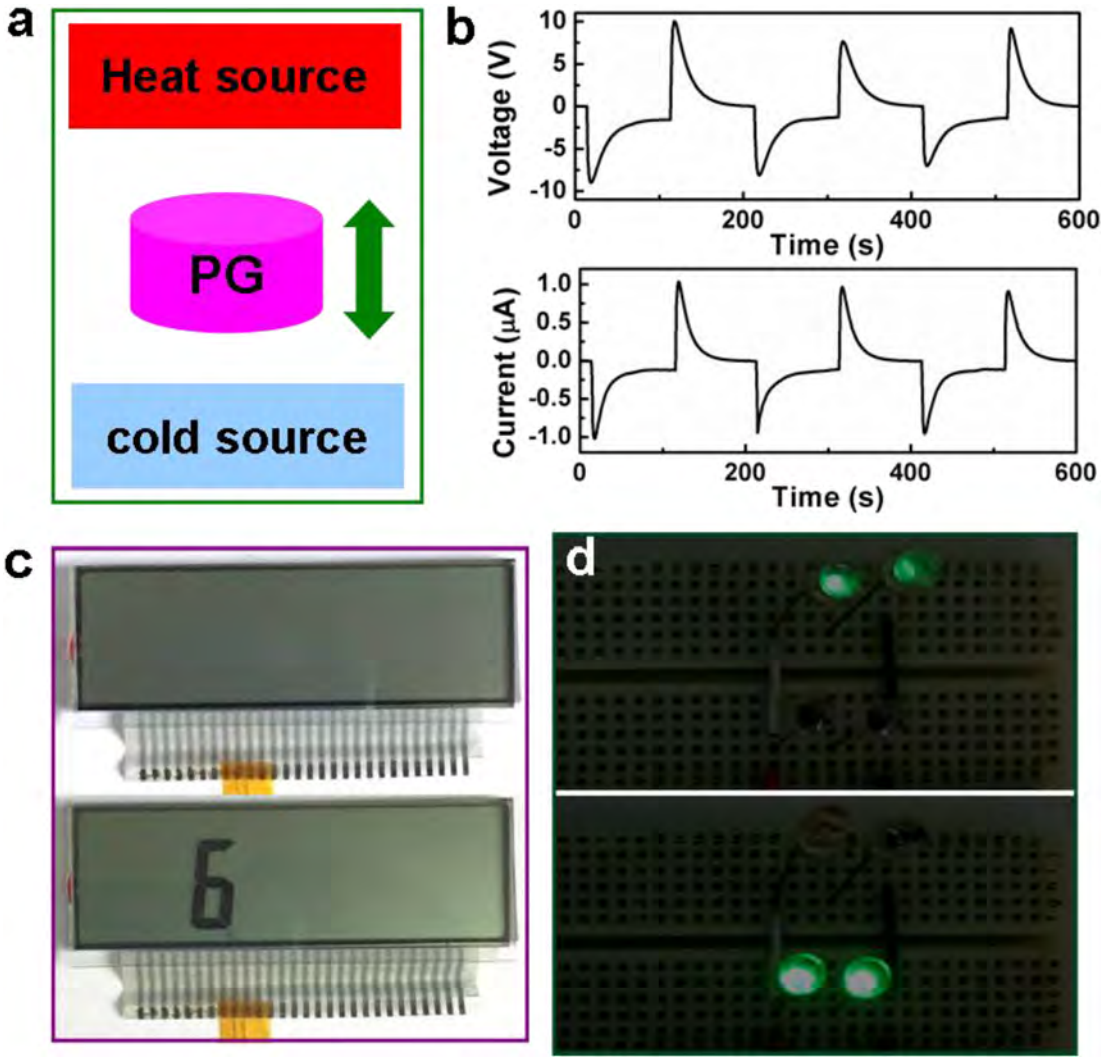

Fig. 6. The verification of the PG used as a direct power source. (a) The schematic diagram of the operation. (b) The output voltage and current of the PG under the forward connection. (c) The optical image of the LCD drove by the PG with number "6" displayed. (d) The photograph of two lines of LEDs lighted up alternately.

experimental data, we can evaluate the approximate pyroelectric coefficient of the PVDF film, which is very close to the performance specifications provided by the manufacturers. Compared with the pyroelectric coefficient of the reported ZnO and $KNbO_3$ semiconductors, our PVDF film can achieve a much higher value. Similarly, the Pyroelectric voltage (V_P) can be given below:

$$V_P = \frac{pd\Delta T}{\varepsilon_r \varepsilon_0 - \varepsilon_0} \tag{2}$$

Here, p also is the Pyroelectric coefficient and d is the thickness of the PVDF film of the fabricated PG device. ε_0 is the permittivity of the ideal vacuum with ε_r of the relative dielectric constant of the PVDF film. For a certain PG device, the above-mentioned parameters are determined. Exceptionally, ΔT corresponds to the change in temperature. From Eqs. (1) and (2), it is can be concluded that, by increasing the temperature difference, the output voltage of the PG can be enhanced. However, the larger output current can be obtained when the temperature changing rate is improved. The conclusion we got here is very well consistent with the measured experimental data.

To demonstrate the PG can be used as a direct power source, Fig. 6a shows the schematic diagram of the PG in operation, where the PG alternately contacts with the heat source (358 K) and cold source (293 K). The curves of the output voltage and current are shown in Fig. 6b under the forward connection condition, with the reversed output signals depicted in Fig. S2, Supporting information. The maximum voltage and current can reach 10 V and 1 μA around, respectively, under the temperature variation. When the PG contacts with the heat source, a LCD screen can be driven by the PG, as shown in Fig. 6c and movie file 1 (see the Supporting information), exhibiting that a number "6" is clearly displayed compared with that is under the condition without temperature variations. To further verify the output power, LEDs were employed to be tested. Two groups of LEDs connected to the PG with reversed polarity to utilize both the positive and negative electricity, as sketched in Fig. S3, Supporting information. Fig. 6d, movie file 2 and movie file 3 (see the Supporting information) display two lines of LEDs can be directly lighted up by the forward and reversed current, respectively, indicating our PG device indeed can be utilized as a direct power source.

Supplementary movie related to this article can be found at http://dx.doi.org/10.1016/j.energy.2016.02.002.

The storage of the electrical energy is an important application for generators. To confirm the feasibility of the electricity storage, a commercial capacitor (22 μF, 25 V) was selected as an

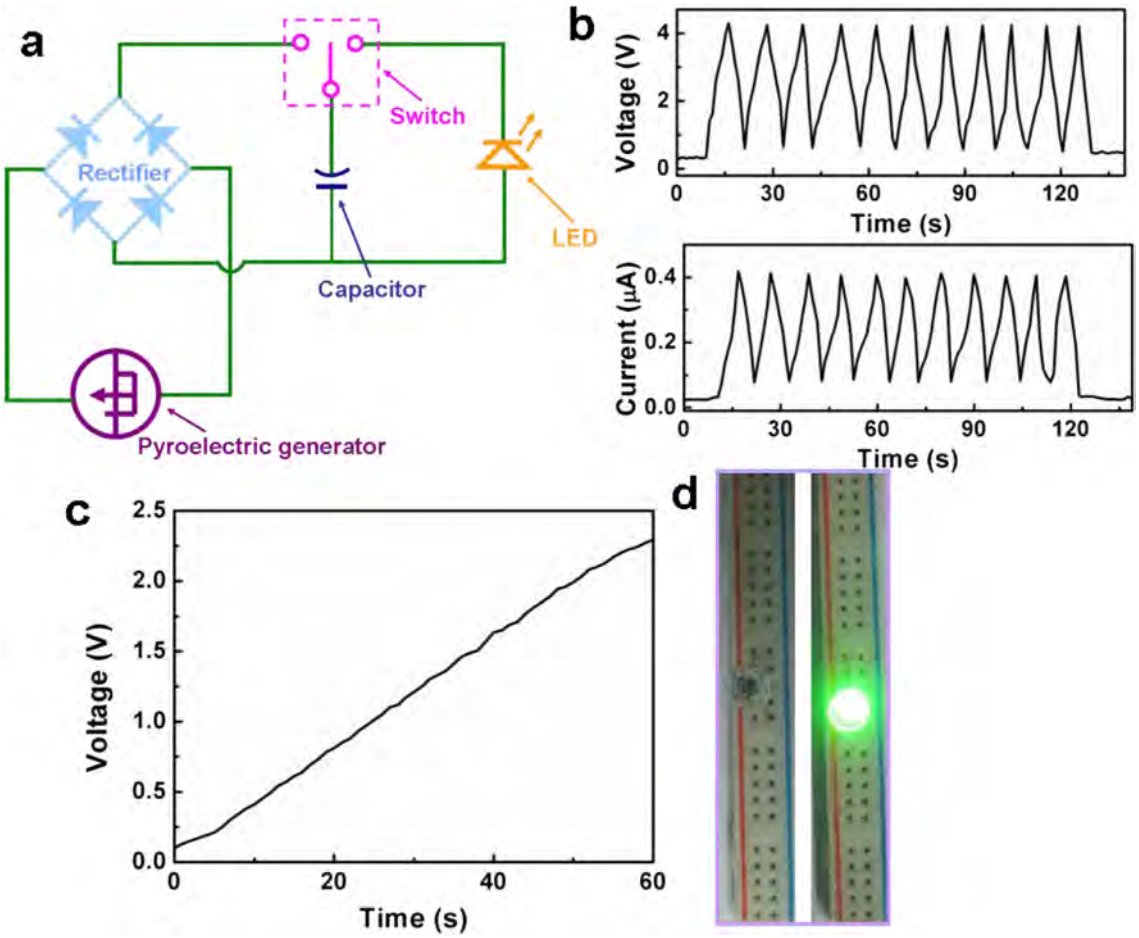

Fig. 7. The charging measurement based on the PG. (a) The circuit diagram of the charging experiment. (b) The rectified output voltage and current of the PG for charging a capacitor. (c) The voltage–time curve of the charged capacitor. (d) The photograph of a LED being driven by the charged capacitor.

energy storage unit. The capacitor was connected to the PG for charging and subsequently was used as a power source for powering LEDs. The circuit diagram is depicted in Fig. 7a. Fig. 7b shows the output performance after rectification of the PG employed for charging experiment. The voltage–time charging curve of the capacitor is recorded in Fig. 7c. Within 60 s, the capacitor was charged from 0.2 V to 2.3 V. Then, the charged capacitor was used as a power source to drive LEDs. Fig. 7d shows a LED is lighted up by the energy stored in the capacitor, with the corresponding video presented in movie file 4 (see the Supporting information).

Supplementary movie related to this article can be found at http://dx.doi.org/10.1016/j.energy.2016.02.002.

To further demonstrate the potential applications of the designed PG device, the PG was utilized as an active self-powered thermosensor. The output voltage of the PG at different temperatures compared with the same original temperature is plotted in Fig. 8a–f. As the temperature goes up, the value of the output signal increases accordingly. The dependence of the output voltage on the temperature and corresponding temperature changing rate is enumerated in Fig. 8g, suggesting an obvious linear relationship between the output voltage and the temperature as well as the temperature changing rate by fitting the data, which is consist with Fig. 3. The excellent linear relationship is beneficial for practical applications of the sensors for detecting the real-time temperature and temperature variation. The response time and reset time are two significant performance indexes for the sensors. By enlarging the output voltage curve when the sensor contacted to the heat source of 353 K, it can be seen that the response time is about 4.8 s, as shown in Fig. 8h. When the sensor was moved out from the heat source, a positive pulse was observed. Fig. 8i reveals the magnified output signal with an exponential decay. The reset time is defined as the time taken to recover to 1/e of the maximum value [23]. By calculation, the reset time is obtained of about 11 s here. The achieved response time and reset time of the PG-based device are desirable for the thermosensors.

4. Conclusion

In summary, a flexible PG device has been fabricated using a PVDF film. It is demonstrated that the PG can be used to harvest thermal energy arising from the time-dependent fluctuating temperature with spatial uniformity. The performance of the PG has been explored in detail, indicating the PG can deliver the output power of about 2.2 μW on a load of 0.1 MΩ at the temperature difference of 50 K. The generated electrical energy by the PG can directly light up a LCD or LEDs, or be stored in a capacitor for subsequent usages. Due to the linear relationship between the output voltage and the temperature as well as the temperature changing rate, the PG has been used as a self-powered thermosensor. The designed PG deice has the potential applications in the ambient thermal energy harvesting from the irregularly shaped or mobile heat source and the self-

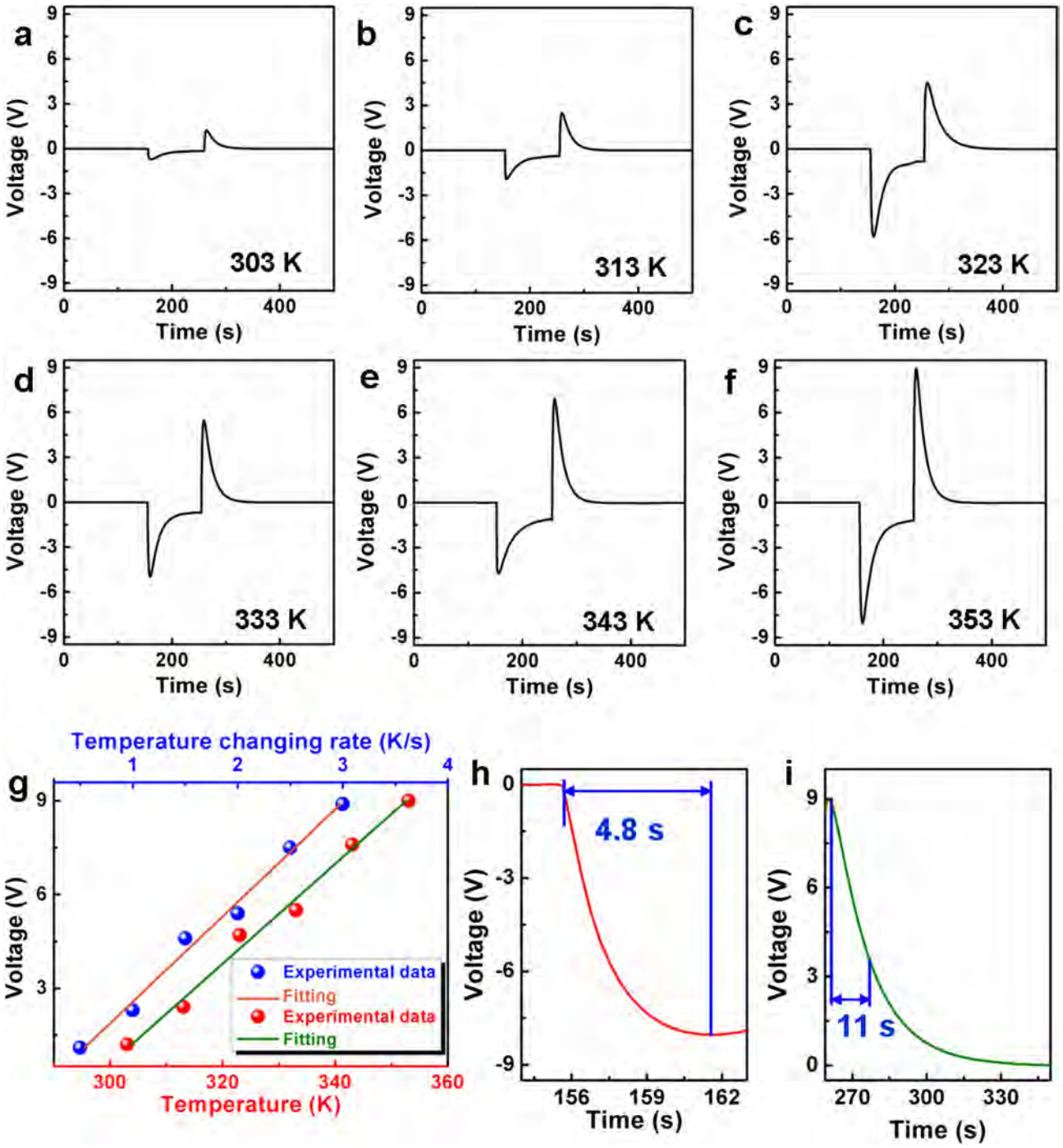

Fig. 8. The demonstration of the PG as a self-powered thermosensor. (a–f) Output voltage under different temperatures of the heat source. (g) Dependence of the output voltage on the temperature and the temperature changing rate. (h) The magnified voltage–time curve of the negative output voltage pulse in panel f. (i) The enlarged positive output signal in panel f.

powered sensing systems, especially in thermal-to-electrical conversion.

Acknowledgements

This work was funded by the National Basic Research Program of China (973 Program) under Grant No. 2015CB351905, National Natural Science Foundation of China (No. 61504019), China Postdoctoral Science Foundation, and Scientific Research Start-up Foundation of University of Electronic Science and Technology of China (Y02002010301082).

Appendix A. Supplementary data

Supplementary data related to this article can be found at http://dx.doi.org/10.1016/j.energy.2016.02.002.

References

[1] Disalvo FJ. Thermoelectric cooling and power generation. Science 1999;285:703–6.
[2] Bell LE. Cooling, heating, generating power, and recovering waste heat with thermoelectric systems. Science 2008;321:1457–61.

[3] Yang Y, Lin Z-H, Hou T-C, Zhang F, Wang ZL. Nanowire-composite based flexible thermoelectric nanogenerators and self-powered temperature sensors. Nano Res 2012;5:888–95.
[4] Hagelstein PL, Kucherow Y. Enhanced figure of merit in thermal to electrical energy conversion using diode structures. Appl Phys Lett 2002;81:559–61.
[5] Lang SB. Pyroelectricity: from ancient curiosity to modern imaging tool. Phys Today 2005;58:31–6.
[6] Ye CP, Tamagawa T, Polla DL. Experimental studies on primary and secondary pyroelectric effects in Pb(Zr x Ti1−x)O3, PbTiO3, and ZnO thin films. J Appl Phys 1991;70:5538–43.
[7] Yang Y, Guo W, Pradel KC, Zhu G, Zhou Y, Zhang Y, et al. Pyroelectric nanogenerators for harvesting thermoelectric energy. Nano Lett 2012;12:2833–8.
[8] Yang Y, Jung JH, Yun BK, Zhang F, Pradel KC, Guo WX, et al. Flexible pyroelectric nanogenerators using a composite structure of lead-free $KNbO_3$ nanowires. Adv Mater 2012;24:5357–62.
[9] Yang Y, Wang S, Zhang Y, Wang ZL. Pyroelectric nanogenerators for driving wireless sensors. Nano Lett 2012;12:6408–13.
[10] Ravindran SKT, Huesgen T, Kroener M, Woias P. A self-sustaining micro thermomechanic-pyroelectric generator. Appl Phys Lett 2011;99:104102.
[11] Ko YJ, Yun BK, Jung JH. A $0.7Pb(Mg_{1/3}Nb_{2/3})O_3$-$0.3PbTiO_3$-based pyroelectric generator and temperature sensor. J Korean Phys Soc 2015;66:713–6.
[12] Leng Q, Chen L, Guo HY, Liu JL, Liu GL, Hu CG, et al. Harvesting heat energy from hot/cold water with a pyroelectric generator. J Mater Chem A 2014;2:11940–7.
[13] Poncharal P, Wang ZL, Ugarte D, De Heer WA. Electrostatic deflections and electrochemical resonances of carbon nanotubes. Science 1999;283:1513–5.
[14] Gao R, Strehle S, Tian B, Cohen-Karni T, Xie P, Duan X, et al. Outside looking in: nanotube transistor intracellular sensors. Nano Lett 2012;12:3329.
[15] Xie P, Xiong Q, Fang Y, Qing Q, Lieber CM. Local electrical potential detection of DNA by nanowire-nanopore sensors. Nat Nanotechnol 2012;7:119–25.
[16] Wu JM, Chen C-Y, Zhang Y, Chen K-H, Yang Y, Hu Y, et al. Ultrahigh sensitive piezotronic strain sensors based on a $ZnSnO_3$ nanowire/microwire. ACS Nano 2012;6:4369–74.
[17] Bergfield JP, Story SM, Stafford RC, Stafford CA. Probing Maxwell's demon with a nanoscale thermometer. ACS Nano 2013;7:4429–40.
[18] Aguilar JLC, Gentle AR, Smith GB, Chen D. A method to measure total atmospheric long-wave down-welling radiation using a low cost infrared thermometer tilted to the vertical. Energy 2015;81:233–44.
[19] Xu S, Qin Y, Xu C, Wei Y, Yang R, Wang ZL. Self-powered nanowire devices. Nat Nanotechnol 2010;5:366–73.
[20] Wang ZL. Toward self-powered sensor networks. Nano Today 2010;5:512–4.
[21] Lang SB, Tofail SAM, Gandhi AA, Gregor M, Wolf-Brandstetter C, Kost J, et al. Pyroelectric, piezoelectric, and photoeffects in hydroxyapatite thin films on silicon. Appl Phys Lett 2011;98:123703.
[22] Tien NT, Seol YG, Dao LHA, Noh HY, Lee NE. Utilizing highly crystalline pyroelectric material as functional gate dielectric in organic thin-film transistors. Adv Mater 2009;21:910–5.
[23] Yang Y, Pradel KC, Jing Q, Wu JM, Zhang F, Zhou Y, et al. Thermoelectric nanogenerators based on single Sb-doped ZnO micro/nanobelts. ACS Nano 2012;6:6984–9.